Downloaded from rstb.royalsocietypublishing.org

PHILOSOPHICAL TRANSACTIONS OF THE ROYAL SOCIETY B BIOLOGICAL SCIENCES

The Aerodynamics of Hovering Insect Flight. V. A Vortex Theory

C. P. Ellington

Phil. Trans. R. Soc. Lond. B 1984 **305**, 115-144
doi: 10.1098/rstb.1984.0053

References Article cited in:
http://rstb.royalsocietypublishing.org/content/305/1122/115.citation#related-urls

Email alerting service Receive free email alerts when new articles cite this article - sign up in the box at the top right-hand corner of the article or click **here**

To subscribe to *Phil. Trans. R. Soc. Lond. B* go to: **http://rstb.royalsocietypublishing.org/subscriptions**

This journal is © 1984 The Royal Society

Downloaded from rstb.royalsocietypublishing.org

Phil. Trans. R. Soc. Lond. B **305**, 115–144 (1984) [115]
Printed in Great Britain

THE AERODYNAMICS OF HOVERING INSECT FLIGHT. V. A VORTEX THEORY

By C. P. ELLINGTON
Department of Zoology, University of Cambridge, Downing Street, Cambridge CB2 3EJ, U.K.

(*Communicated by Sir James Lighthill, F.R.S.* – *Received* 28 *March* 1983)

CONTENTS

A full derivation is presented for the vortex theory of hovering flight outlined in preliminary reports. The theory relates the lift produced by flapping wings to the induced velocity and power of the wake. Suitable forms of the momentum theory are combined with the vortex approach to reduce the mathematical complexity as much as possible.

The Royal Society is collaborating with JSTOR to digitize, preserve, and extend access to *Philosophical Transactions of the Royal Society of London. Series B, Biological Sciences.* www.jstor.org

Downloaded from rstb.royalsocietypublishing.org

Vorticity is continuously shed from the wings in sympathy with changes in wing circulation. The vortex sheet shed during a half-stroke convects downwards with the induced velocity field, and should be approximately planar at the end of a half-stroke. Vorticity within the sheet will roll up into complicated vortex rings, but the rate of this process is unknown. The exact state of the sheet is not crucial to the theory, however, since the impulse and energy of the vortex sheet do not change as it rolls up, and the theory is derived on the assumption that the extent of roll-up is negligible. The force impulse required to generate the sheet is derived from the vorticity of the sheet, and the mean wing lift is equal to that impulse divided by the period of generation. This method of calculating the mean lift is suitable for unsteady aerodynamic lift mechanisms as well as the quasi-steady mechanism.

The relation between the mean lift and the impulse of the resulting vortex sheet is used to develop a conceptual artifice – a pulsed actuator disc – that approximates closely the net effect of the complicated lift forces produced in hovering. The disc periodically applies a pressure impulse over some defined area, and is a generalized form of the Froude actuator disc from propeller theory. The pulsed disc provides a convenient link between circulatory lift and the powerful momentum and vortex analyses of the wake.

The induced velocity and power of the wake are derived in stages, starting with the simple Rankine–Froude theory for the wake produced by a Froude disc applying a uniform, continuous pressure to the air. The wake model is then improved by considering a 'modified' Froude disc exerting a continuous, but non-uniform pressure. This step provides a spatial correction factor for the Rankine–Froude theory, by taking into account variations in pressure and circulation over the disc area. Finally, the wake produced by a pulsed Froude disc is analysed, and a temporal correction factor is derived for the periodic application of spatially uniform pressures. Both correction factors are generally small, and can be treated as independent perturbations of the Rankine–Froude model. Thus the corrections can be added linearly to obtain the total correction for the general case of a pulsed actuator disc with spatial and temporal pressure variations.

The theory is compared with Rayner's vortex theory for hovering flight. Under identical test conditions, numerical results from the two theories agree to within 3%. Rayner presented approximations from his results to be used when applying his theory to hovering animals. These approximations are not consistent with my theory or with classical propeller theory, and reasons for the discrepancy are suggested.

1. Introduction

The essence of flight is that wings impart downward velocity and momentum to the air, and obtain a lift force by reaction. This downward air velocity – the induced velocity – influences the relative airflow over the wings and hence their lift. For detailed calculations of the lift force resulting from a given wing motion, some relation must be established between the induced velocity and the lift. Furthermore, a substantial expenditure of energy per unit time is needed to impart downward momentum to the air – the induced power requirement – and a relation between the downward air motion and lift is also necessary to calculate this power.

Two theories, incomplete in themselves, together provide an approximate basis for the conventional aerodynamic analysis of flapping flight. As discussed in paper I, this analysis is composed of a force coefficient blade-element theory and a momentum theory. The wings are divided into blade elements perpendicular to the span, and the instantaneous lift and profile drag for each element are calculated from the force coefficients corresponding to the instantaneous airflow around the element. The induced velocity component of the airflow is

Downloaded from rstb.royalsocietypublishing.org

obtained from a momentum theory, by equating the lift force required for flight to the rate of change of momentum necessarily imparted to the air. As a corollary to the momentum theory, the induced power is usually estimated from the kinetic energy flux of the downward air motion. The general equations for this aerodynamic analysis were first derived by Osborne (1951) for flapping insect flight, and a similar treatment is also employed for bird flight (Pennycuick 1968, 1975; Tucker 1973). Such analyses invoke the quasi-steady approximation, and assume that the force coefficients at any instant are those corresponding to steady motion at the same instantaneous relative air velocity (paper I). The quasi-steady assumption is not essential for the analysis, however: force coefficients can be defined for unsteady as well as steady motion.

For the most complete physical and analytical description of lift, we must turn to a vortex theory of flight. The lift of a wing, and hence the lift coefficient, is governed by the circulation of bound vorticity (paper IV). Vorticity is shed into the passing air as the lift and circulation change during flight, and forms a vortex wake that corresponds to the downward air motion treated by the momentum approach. By using the concept of circulation a vortex theory thus relates the induced velocity to the wing lift, and unifies the two previous theories in a single framework.

Vortex theories are not a new approach to animal flight mechanics. Cone (1968) first presented a detailed discussion of the vortex wake produced by the flapping wings of an animal. He developed the general equations for a vortex theory of flapping flight, but they proved too cumbersome for practical application. Betteridge & Archer (1974) simplified the three dimensional geometry and kinematics, and invoked the quasi-steady assumption, resulting in a manageable vortex theory for fast flapping flight. Ellington (1978) reviewed the existing theories for hovering flight and outlined a simplified vortex theory following in the wake, so to speak, of classical propeller theories five decades old. More details of the theory were given in Ellington (1980), including a novel correction for the energy losses associated with periodicity of the vortex wake structure – the 'tip losses' of propellers. Vortex theories of hovering and forward flight have also been developed by Rayner (1979*a*, *b*), and are summarized in Rayner (1979*c*).

The vortex theories of Ellington and Rayner are but partially complete. They provide a method of calculating the *mean* lift and induced power for a given circulation profile during the wingbeat – the circulation as a function of spanwise position and time – for unsteady as well as quasi-steady aerodynamic mechanisms. However, the induced velocity is not added to the wing motion to estimate the resulting unsteady circulation and instantaneous lift. The theories therefore rely on *postulated* circulation profiles instead of actually solving for the profile consistent with the wing motion. The justification for this approach is that measurements of the angle of attack and camber for the wing elements are extremely scarce, so details of the wing motion itself are not sufficiently known in most cases. Instead of assuming a given circulation profile, Phlips *et al.* (1981) assumed a simple wing motion, and were the first to succeed in developing a full unsteady vortex theory for flapping flight with specified kinematics. They ignored the downward movement of vorticity in the wake, which is a reasonable approximation for fast forward flight, but this prevents application of their theory to slow and hovering flight.

Although a complete vortex theory is obviously desirable for a study of hovering flight, it is not possible at present. Given the inadequate kinematic data, an assumption must be made either about the circulation profile or the wing motion. It is most probable that a complete

Downloaded from rstb.royalsocietypublishing.org

theory must also include the effects of leading edge vortex shedding during the wingbeat (paper IV). Our knowledge about vortex shedding from sharp leading edges, and the subsequent formation and stability of leading edge bubbles, is very limited, and much experimental work must be done before these effects can be incorporated into a complete theory. For the present, it thus seems more appropriate to postulate how the circulation around the wing elements is likely to vary during hovering flight, based on the discussions of paper IV. The vortex theory of Ellington (1978, 1980) was designed to calculate the mean lift and induced power for such circulation profiles, and will therefore be used in paper VI to provide estimates for the insects of this study. Although the theory could only be outlined in the earlier publications, it forms an integral part of this work and so is presented here in detail. Rayner (1979*a*, *c*) did not draw comparisons between his vortex theory for hovering flight and mine of 1978, and my treatment of wake periodicity was published just after his papers, so a comparison of the two theories will also be given.

2. The mean lift

In this section, the first part of the vortex theory, equations are derived for the mean circulatory lift produced by the flapping wings in hovering flight. The analytical procedure is identical to that for the blade-element theory which was discussed in papers I and IV. It is assumed that the total force on a wing is the sum of the forces acting on a number of spanwise *wing elements*, each of which can be represented by a two dimensional aerofoil experiencing a relative velocity composed of the flapping velocity and the induced velocity of wake vorticity. Knowledge of the induced velocity is taken for granted in developing the equations of this section, but the actual derivation of it cannot be achieved until the second part of the theory.

Thoughout the theory, it will be assumed that the wing motion is confined to the stroke plane. This is not a necessary assumption, but it greatly simplifies the mathematics without introducing serious errors.

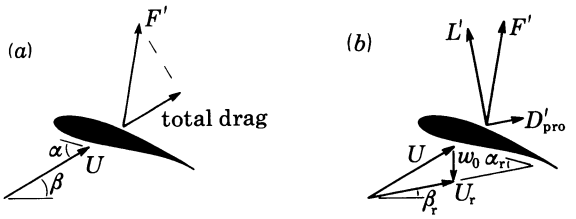

Figure 1. (*a*) Kinematic definitions and the net aerodynamic force F' on a wing element. The *total drag* is referred to in the second part of the theory. (*b*) Resolution of F' into circulatory lift L' and profile drag D'_{pro} with respect to the relative velocity U_r, which is given by the vector sum of the flapping velocity U and the induced velocity w_0.

Figure 1*a* shows a wing element at that moment in the downstroke when the wing span is horizontal: that is, the positional angle ϕ is zero according to the kinematic definitions in paper III. The flapping velocity U is at the stroke plane angle β to the horizontal, and the geometrical angle of attack is α. The wing element produces a net aerodynamic force F', where the prime notation again denotes a force per unit span. The motion of the wing element relative to the air is given by the vector sum of the flapping velocity U and the induced velocity w_0 of vorticity in the wake (figure 1*b*). As will be shown later, this induced velocity must be very close to vertical in hovering. The relative velocity U_r experienced by the wing element thus makes a

Downloaded from rstb.royalsocietypublishing.org

smaller angle β_r to the horizontal than does the flapping velocity, and the angle of attack of the relative wind α_r is similarly reduced to $\alpha-(\beta-\beta_r)$.

The aerodynamic forces produced by the element are determined by the direction and magnitude of the relative velocity, so the net force F' is usually resolved into components relative to U_r. The force component parallel to U_r is the profile drag of the element D'_{pro}, and that perpendicular to U_r is the circulatory lift L'. The discussion of aerodynamic mechanisms in paper IV emphasized the bound vorticity of the wing necessary for circulatory lift, but pointed out the problems in actually calculating the *instantaneous* lift from the linearized equations of unsteady aerofoil theory. This difficulty is partially resolved by the vortex theory, which derives the *mean* circulatory lift from the *wake vorticity* that must be shed as the wing circulation changes during the cycle. Bound and wake vorticity are related, of course, so we are just looking at the same problem from a different viewpoint.

2.1. *The vortex sheet from circulatory lift*

Figure 2*a* shows the vortex wake created by the changes in circulation around a pair of wings during a half-stroke. The wing circulation Γ measures the strength of the bound vorticity, which may vary with radial position r along the wing and with time t. As discussed in paper IV,

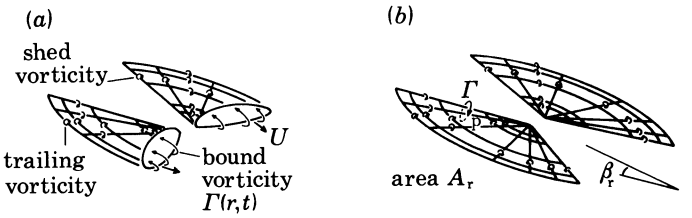

FIGURE 2. (*a*) Creation of the vortex sheet corresponding to changes in circulation around wing elements during a half-stroke. (*b*) At the end of the half-stroke the resultant vortex sheet is approximately planar, forming an angle β_r with the horizontal.

'starting' or 'stopping' vorticity must be shed from the trailing edge of each wing element in sympathy with any changes in circulation during the half-stroke. This 'shed vorticity', of strength $-(\partial\Gamma/\partial t)\,dt$, is deposited along radial paths in the 3-dimensional motion of hovering. If the circulation also changes between wing elements at r and $r+dr$, then 'trailing vorticity' of strength $-(\partial\Gamma/\partial r)\,dr$ must be passed into the wake. This vorticity is laid down tangential to the wing motion and thus forms circular vortex lines in hovering: it corresponds to the trailing, or tip, vortices produced by conventional aeroplane wings. Trailing vorticity does not enter into the consideration of two dimensional aerofoils, for which the circulation is constant along the infinite span, but it must be produced by real wings. Even if the circulation is constant along a wing of finite span it must fall to zero at the ends of the wing, and trailing vortices will be created there. At the end of the half-stroke the remaining bound vorticity is shed, freeing the vortex sheet from the wing (figure 2*b*). The net result of the wing action is, therefore, the generation of a vortex sheet with continuously distributed radial and tangential vorticity.

After each region of the sheet is created, it moves downwards because of the induced velocity of the wake vorticity. Thus the final form of the sheet is governed by the fact that elements of vorticity shed near the beginning of the half-stroke convect downwards a greater distance than those shed near the end. The induced velocity may vary over the cycle, and the resulting

Downloaded from rstb.royalsocietypublishing.org

three dimensional vortex sheet will form a limited area on some irregular helicoid. However, an approximation can be invoked to reduce the geometrical complexity of the sheet. Results from paper VI show that the induced velocity is substantially smaller in general than the flapping velocity, so regions of the sheet can move but a short distance during the half-stroke. The resulting helicoidal sheet is only slightly developed, therefore, and may be considered as approximately planar: although an entire helicoid cannot be represented by a plane, limited areas of it can be without serious distortion. The plane containing the vortex sheet is parallel to the mean relative velocity of the wings, and the angle between this plane and the horizontal can be denoted by the *relative stroke plane angle* β_r (figure 2*b*). The area swept by the wings in the stroke plane is ΦR^2, where Φ is the stroke angle in radians and R is the wing length, and the area A_r of the vortex sheeet in the relative stroke plane must equal $\Phi R^2 \cos\beta/\cos\beta_r$ if the induced velocity w_0 is vertical.

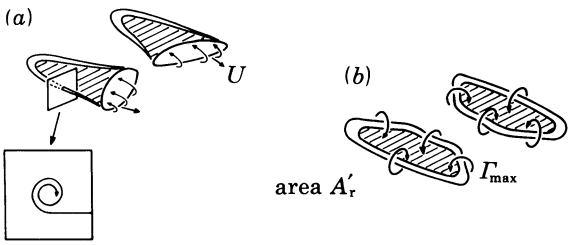

FIGURE 3. (*a*) Roll-up of the vortex sheet during a half-stroke. The vorticity rolls up into a core around the perimeter. (*b*) All of the vorticity created during the half-stroke is shown concentrated into two 'rings' enclosing a total area A'_r. The circulation of each ring is Γ_{max}.

A vortex sheet is unstable and will roll up at the edges under the influence of its own induced velocity field. This phenomenon is well known for the 'horseshoe' vortex system behind conventional aeroplane wings: the vorticity shed at the beginning of motion rolls up into a concentrated starting vortex, and the trailing vorticity rolls up into two discrete tip vortices about 13 chord lengths behind the wing (Milne-Thomson 1973). The rate of roll-up is not known, however, for the vortex sheet created during a half-stroke. Figure 3 shows the extreme case where the sheet rolls up almost as soon as it is generated. This results in two irregular vortex 'rings' at the end of the half-stroke. All of the vorticity produced by the wings must be concentrated around the perimeter of these rings, enclosing a total area A'_r which is less than the sheet area A_r. It is likely that a viscous *core* containing the rolled-up vorticity develops around the ring perimeter, but the exact shape of this core and the distribution of vorticity within it are not known. The actual state of the vortex sheet will be somewhere between completely rolled-up rings at one extreme and a planar sheet at the other. Fortunately, the impulse and energy of a vortex sheet in an inviscid fluid do not change with rolling up, so the exact state of the sheet will not affect the theory.

In his three dimensional flow visualization experiments on the fling mechanism, Maxworthy (1979) observed the formation of well-defined tip vortices during the half-stroke. These vortices were very similar to those around delta wings at high angles of incidence: the 'bound' vorticity moved axially along the leading edge separation vortex produced by the fling, and was deposited in the wake as a strong tip vortex. Maxworthy suggests that this spanwise transport of vorticity stabilizes the leading edge vortex bubble, and therefore prevents the abrupt loss of fling circulation by the usual two dimensional stalling. This interpretation is consistent with

Downloaded from rstb.royalsocietypublishing.org

the known characteristics of delta flows, and it may apply more generally to the leading edge bubbles expected around the wings of insects, bats and some birds (paper IV). More three dimensional flow visualization experiments are obviously desirable to resolve this point, and the information they provide on the rate of rolling up would also be useful.

2.2. *Impulse of the vortex sheet*

The vortex sheet is a surface of discontinuity, or separation, in the air. Any vorticity created by the wings must be confined to that thin layer where the air passing over the wing is rejoined with that passing under it. The air surrounding the sheet contains no vorticity, which can be created only at the interface between the air and a solid object, thus the surrounding air is in *irrotational* motion. The velocity potential ϕ_v of the fluid motion must be continuous throughout the irrotational flow, but a discontinuity of some magnitude $\Delta\phi_v$ exists across the sheet. The same flow field can, in fact, be generated by a hypothetical mechanism that is divorced from the wing action – the application of an *impulsive pressure* to the surface of separation. By considering the impulse that would produce an identical flow pattern, a technique sometimes employed in fluid dynamics (Prandtl & Tietjens 1957*b*; Kármán & Burgers 1935), the mean circulatory force applied to the air by the beating wings can be estimated.

The concept is described in the following way. The sheet of discontinuity is replaced by a rigid surface in air at rest. This surface then exerts a pressure p on the air for a very brief period τ, and the time integral of the pressure over this period equals the pressure impulse. At the end of the period the irrotational flow around the surface is the same as that around the vortex sheet created by the wings, and the rigid surface immediately disappears. The pressure impulse also generates vorticity over its surface of application (Kármán & Burgers, 1935) and, if the irrotational motions are identical, then the vortex sheet produced by this mechanism must be equivalent to that created by the wings. Because the resulting air motions are equal, the impulse applied by either mechanism will be the same.

The discontinuity $\Delta\phi_v$ in the velocity potential across a small area dA of the sheet can be produced by the application of a pressure impulse equal to $\rho\Delta\phi_v$, where ρ is the density of air. The *force impulse* dI corresponding to this pressure impulse is $\rho\Delta\phi_v\,dA$, and the direction of the applied force must be perpendicular to the area dA. It should be noted that this impulse is independent of any other vorticity in wake: the flow associated with other vorticity must be irrotational in the region of the area dA and cannot introduce a discontinuity in the velocity potential there. The *total impulse* I required to generate the surface of discontinuity is obtained by integrating the force impulse over the area of the sheet. This is a vector operation in general, but because the vortex sheet is approximately planar we can simply write

$$I = \rho \iint_{A_r} \Delta\phi_v \, dA, \tag{1}$$

where the net force impulse is perpendicular to the relative stroke plane.

The circulation Γ around any closed curve in a fluid is defined as the line integral of the fluid velocity along the curve. If the curve is limited to irrotational regions of flow, then the line integral and the circulation are both zero. Now consider the curve intersecting the vortex sheet at point p in figure 2*b*. The curve lies in irrotational flow except for the intersection, so the circulation around the curve must equal the local discontinuity of the velocity potential $\Delta\phi_v$ across the sheet. From the figure it is clear that Γ must also equal the strength of all the

Downloaded from rstb.royalsocietypublishing.org

vortex lines between p and the sheet boundary. These vortex lines are just the shed vorticity $-(\partial\Gamma/\partial t)\,\mathrm{d}t$ of the wing, so the sum of the vorticity enclosed by the curve must equal the circulation Γ around the wing as it passed the point in the stroke plane corresponding to p on the sheet. Equation (1) can now be transformed into an integral of the wing circulation over the area swept by the wings using the definition of A_r and the relation between Γ and the discontinuity in the velocity potential:

$$I = 2\rho\frac{\cos\beta}{\cos\beta_\mathrm{r}}\int_{\phi_\mathrm{min}}^{\phi_\mathrm{max}}\int_0^R \Gamma r\,\mathrm{d}r\,\mathrm{d}\phi, \tag{2}$$

where Γ is the circulation around the wing element at r when the positional angle of the wing is ϕ (the regrettable double usage of this symbol arises from conventions in fluid mechanics and the descriptive geometry for wing motion).

It will prove useful to introduce a non-dimensional wing circulation $\hat{\Gamma}$, given by the ratio of Γ to the maximum circulation Γ_max around the wing during the half-stroke. This normalizes the circulation profile, or distribution, over the sheet with $\hat{\Gamma}$ ranging between 0 and 1. For a given profile, the net impulse is then proportional to the maximum circulation Γ_max. It is also advantageous to integrate equation (1) over a non-dimensional area so that the impulse is proportional to the area of the sheet A_r. This can be done with the non-dimensional parameters of wing position defined in paper III; the positional angle ϕ of the wing in the stroke plane is replaced by $\hat{\phi}$, which varies between 1 and -1, and the radial position r of a wing element is divided by R to give $\hat{r}$. Equation (2) can then be written as

$$I = \rho\Phi R^2\frac{\cos\beta}{\cos\beta_\mathrm{r}}\Gamma_\mathrm{max}\int_{-1}^{1}\int_0^1 \hat{\Gamma}\hat{r}\,\mathrm{d}\hat{r}\,\mathrm{d}\hat{\phi}, \tag{3}$$

$$I = \rho A_\mathrm{r}\Gamma_\mathrm{max}\hat{I}. \tag{4}$$

Although equations (2) and (3) are more directly related to events in the stroke plane, equation (4) offers a better physical interpretation of the impulse of the vortex sheet: the impulse is proportional to the product of air density, area and maximum circulation of the sheet. The constant of proportionality, $\hat{I}$, may be regarded as a non-dimensional impulse and is solely determined by the normalized distribution of circulation over the sheet:

$$\hat{I} = \int_{-1}^{1}\int_0^1 \hat{\Gamma}\hat{r}\,\mathrm{d}\hat{r}\,\mathrm{d}\hat{\phi}. \tag{5}$$

This definition also shows that $\hat{I}$ is equivalent to the mean value of $\hat{\Gamma}$ over the *area* of the sheet, $\bar{\hat{\Gamma}}$, and this value must lie between 0 and 1.

The impulse of the vortex sheet does not change when it rolls up into two discrete vortex rings. The area A_r' of the rings can therefore be calculated by equating their impulse to that of the planar vortex sheet. Because all of the sheet vorticity is concentrated around the perimeters, the circulation of any curve intersecting the area enclosed by the rings is constant and equal to Γ_max (figure 3*b*). Thus the impulse of the rings is simply $\rho A_\mathrm{r}'\Gamma_\mathrm{max}$ and, using equation (4), the rolled-up area A_r' is equal to $A_\mathrm{r}\hat{I}$.

2.3. *Mean circulatory lift*

The force impulse required to generate the vortex sheet must be provided by the wings, and is equal to the time integral of the circulatory lift over the duration of the half-stroke. The *mean*

Downloaded from rstb.royalsocietypublishing.org

circulatory lift $\bar{L}$ is therefore given by the impulse divided by that period. The period is not equivalent to the duration τ of the impulse, incidentally; the derivation of the impulse theory from Bernoulli's general equation for unsteady motion requires that τ is infinitesimally brief (Prandtl & Tietjens 1957*b*). If n is used to denote the wingbeat frequency, $\bar{L}$ is simply equal to $2nI$ over a half-stroke and an appropriate expression for I can be chosen from above. The direction of the mean circulatory lift is, by definition, perpendicular to the relative stroke plane.

For some applications it is more convenient to consider the circulation around a wing element as a function of time instead of the positional angle of the wing. The order of integration may be reversed in equation (2), and $r\,\mathrm{d}\phi$ can then be written as $r(\mathrm{d}\phi/\mathrm{d}t)\,\mathrm{d}t = U\,\mathrm{d}t$, where U is the flapping velocity. With this substitution, the mean circulatory lift is equal to

$$\bar{L} = 2\rho \frac{\cos\beta}{\cos\beta_r} \int_0^R \overline{U\Gamma}\,\mathrm{d}r, \tag{6}$$

where $\overline{U\Gamma}$ for a wing element is the mean value of the product of its flapping velocity and circulation. Thus the mean circulatory lift on a particular span-wise element must be

$$\overline{L'} = \rho \frac{\cos\beta}{\cos\beta_r} \overline{U\Gamma}, \tag{7}$$

and equation (6) is just the sum of this quantity for all of the wing elements. Equation (7) can, in fact, be interpreted as the mean of the product of Γ and a velocity given by $U\cos\beta/\cos\beta_r$, since $\cos\beta$ and $\cos\beta_r$ are taken as constant during the half-stroke. After some rather tedious vector analysis, it can be shown that this velocity is actually the relative velocity component perpendicular to the span of the wing. As stated in paper I, any spanwise component of the relative velocity is assumed to have no effect on the aerodynamic force produced by a wing element, so the relative velocity U_r that governs the circulatory lift on an element is more properly equal to this perpendicular component,

$$U_r = U\cos\beta/\cos\beta_r, \tag{8}$$

and equation (7) can now be written as

$$\overline{L'} = \rho\,\overline{U_r\Gamma}. \tag{9}$$

This useful result, which I have not seen elsewhere, provides a form of the Kutta–Joukowski theorem applicable to unsteady aerodynamics. The circulatory lift on an element in steady motion is equal to $\rho U_r \Gamma$ according to the theorem, but this expression cannot be used to calculate the instantaneous lift in unsteady motion (paper IV). Equation (9), however, shows that the *mean* circulatory lift is given by the mean value of the Kutta–Joukowski relation even for unsteady motion. This result is valid only for the assumptions of this vortex theory of hovering, but a general proof of equation (9) for arbitrary unsteady motions is easily derived in the same manner.

2.4. *The pulsed actuator disc*

The essence of hovering is the production of a vertical force to balance the animal's weight. Depending on the relative stroke plane angle β_r, this task can be accomplished using lift, profile drag, or a combination of the two. The final calculations in paper VI reveal that β_r is close to zero for animals hovering with a horizontal stroke plane, thus the circulatory lift of each half-stroke is responsible for weight support: the induced velocity is small with respect to the

Downloaded from rstb.royalsocietypublishing.org

flapping velocity for this group, so β_r does not differ much from β and both angles are quite small. Paper VI also shows that circulatory lift on the downstroke can provide virtually all of the weight support for most animals hovering with an inclined stroke plane. When the induced velocity is added to the flapping velocity of an inclined stroke plane, β_r is less than β on the downstroke but greater than β on the upstroke. The induced velocity is a substantial fraction of the flapping velocity for this group, resulting in a relative stroke plane close to horizontal on the downstroke but strongly inclined on the upstroke. The upstroke cannot produce a significant vertical force without a concomitant large horizontal thrust, therefore the downstroke lift is much more likely to provide the weight support.

The role of circulatory lift for these two groups can be idealized by considering that the mean lift is exactly vertical and is of sufficient magnitude to balance the weight. Two lift impulses per wingbeat provide the weight support for animals hovering with a horizontal stroke plane, but only one impulse is used for an inclined stroke plane: if the frequency of lift impulses is denoted by f, then f equals $2n$ and n respectively. The ideal lift impulse, which shall be called I_0, is therefore vertical and equal to mg/f in order to balance the weight over the period $1/f$ in both groups. The vortex sheet generated by each impulse must be horizontal, and its area A_0 is given by the projection onto the horizontal plane of the area swept by the wings:

$$A_0 = \Phi R^2 \cos \beta. \tag{10}$$

For the sheet impulse to provide the required weight support, the maximum circulation of each sheet must, from equation (4), be given by

$$\Gamma_{\max} = I_0/\rho A_0 \hat{I} = mg/\rho f A_0 \hat{I}. \tag{11}$$

The essential wing action in hovering can therefore be represented by a hypothetical mechanism which periodically applies a pressure impulse mg/fA_0 over the horizontal surface of area A_0 in the air.

An appropriate name for this mechanism is a *pulsed actuator disc* because of its obvious relation to the conceptual device employed in the momentum theory of propellers. In that theory the propeller is replaced by a thin disc, a Froude actuator disc, which applies a *steady* pressure to the air corresponding to the propeller thrust. The Froude disc may be regarded as a special case of the *pulsed* actuator disc because, in the limit, the pulsed disc will produce a steady pressure as the frequency f of impulses becomes infinite.

The pulsed actuator disc is an extremely useful artifice that links the two parts of the vortex theory. As a fitting end to the first part, the disc closely approximates the net effect of the complicated lift forces produced in hovering. These forces must impart momentum to the air according to Newton's laws, and the momentum change takes the form of a jet of air blowing down vertically below the animal. The second part of the theory deals with the characteristics of this jet, particularly the power required to generate it. A complete analysis of the jet is an impossible task, however, and simplifications must be employed. The hypothetical jet which would be produced by the operation of a pulsed actuator disc is, in fact, a very good model for the real jet.

3. The wake

The vortex theory has so far concentrated on the local aerodynamic events around the wings. This near-sighted approach is useful for the analysis of the mean lift, but it cannot be entirely

Downloaded from rstb.royalsocietypublishing.org

satisfactory because the operation of a wing is affected by its past history. Indeed, an ill-defined 'induced velocity' attributable to wake vorticity had to be pulled out of the air to explain some of the local effects. Paper VI shows that the induced velocity is usually small with respect to the flapping velocity, though, and that its effect on the mean lift is negligible for most hovering animals. This does not justify ignoring the induced velocity, however; it is directly responsible for a large *power* expenditure in hovering flight.

Returning briefly to figure 1*a*, the total power required to move a wing element is equal to the flapping velocity U multiplied by the 'total drag' force – the component of the net aerodynamic force F' that is parallel to U. Because the circulatory lift is perpendicular to the relative velocity U_r, which is given by the vector sum of U and the induced velocity w_0, the lift actually contributes an amount $L' \sin(\beta - \beta_r)$ to the total drag. This contribution is determined by the induced velocity and hence is called the *induced drag*: the work done by the wing against the induced drag is, in fact, equal to the energy imparted to the vortex wake. The remainder of the total drag arises from the profile drag of the element. The *total power* required to move the wing is also divided into these two components by convention: *induced power* P_{ind} and *profile power* P_{pro}.

Even though $\sin(\beta - \beta_r)$ may be small because of a 'negligible' induced velocity, when multiplied by the large lift force it can result in a substantial induced power demand. The induced velocity w_0 must therefore be calculated with some accuracy, but it can be derived directly from the induced velocity field of wake vorticity only if the positions and strengths of all vortices are known. The wake is conceptually analogous to that of a propeller, but the distribution of vorticity within it is more complex because of the absence of both axial symmetry and a relatively simple helicoid geometry. These complications may seem formidable when Bramwell (1976) writes of the comparatively simple helicopter wake: 'since the only flow through the rotor in hovering flight is due to the velocity field created by the bound vortices and the vortex sheets, and since the distribution of the vortex sheets is determined by this velocity field, the problem of calculating the flow becomes extremely complicated and a purely analytical solution is out of the question.'

Because of these difficulties, the success of propeller theories rests on a judicious simplification of the wake structure. A similar course will be attempted here, and it relies heavily on an alternative description of the wake that avoids the vorticity distribution altogether. The wings must create a region of low pressure above them and one of high pressure below to support the animal's weight in hovering. The net effect of this is to suck air, initially at rest far above the animal, down towards the wings and then drive it away below. The jet thus formed corresponds to the momentum imparted to the air by the reaction of the wing forces: unless Newton's laws are to be violated, such a jet *must* be produced as a necessary consequence of hovering.

It should be apparent that this *momentum jet* is, in fact, synonymous with the *vortex wake* of the wings. Vorticity shed from the wings convects with the surrounding air, so the vortex wake must be contained within the jet and its motion governed by the jet velocity. The motion of a vortex wake can be determined separately from the induced velocity field of its own vorticity, though, and the two approaches will be consistent only if the air motion of the jet is identical to the induced velocity field of the vortex wake. In particular, the downward velocity of the jet in the vicinity of the beating wings must equal the induced velocity w_0 from the wake vorticity. Furthermore, the rate at which energy is supplied to the jet to increase its momentum

PHILOSOPHICAL TRANSACTIONS OF THE ROYAL SOCIETY B BIOLOGICAL SCIENCES
PHILOSOPHICAL TRANSACTIONS OF THE ROYAL SOCIETY B BIOLOGICAL SCIENCES

Downloaded from rstb.royalsocietypublishing.org

must be equivalent to the power imparted to the vortex wake, which is simply the induced power P_{ind}. By oscillating between these two alternative descriptions of the wake, and their associated analytical techniques, we can develop in stages an improved model for the estimation of induced power and velocity.

3.1. *The Rankine–Froude momentum theory*

The momentum theories of propellers, initiated by Rankine and further developed by Froude, determine the air velocities in the wake from the momentum flux required to provide a given propeller thrust. In the simplest theory, the Rankine–Froude axial momentum theory, the wake is considered as a steady jet with a uniform axial velocity across any cross-sectional area. Although this model is very crude, it actually represents the *ideal* wake for a propeller: the momentum flux required for a given thrust will be produced for the minimum induced power when the wake corresponds to these assumptions. Hoff (1919) first pointed out that this model could also be applied to animal flight studies, and it has been widely used since then to estimate the induced velocity and power in such studies. For practical and historical reasons, the Rankine–Froude theory is therefore the most suitable starting point for a more sophisticated analysis of the wake.

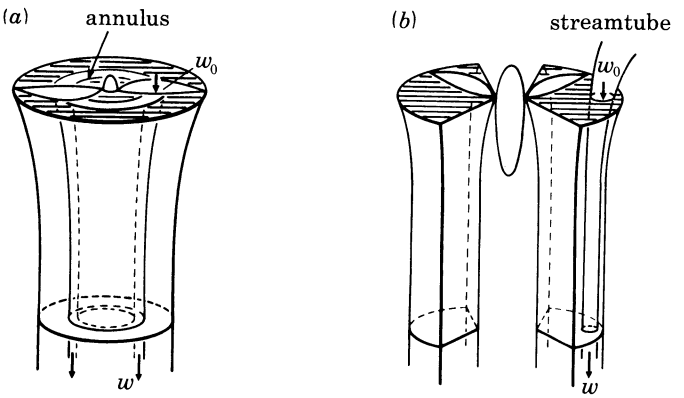

FIGURE 4. The idealized wake flow of the axial momentum theory for a hovering propeller in (*a*) and an animal in (*b*). The actuator disc in each case is indicated by the shaded area. The vertical velocities are constant across the wake in the Rankine–Froude theory, but they may vary between annuli and streamtubes in the differential momentum theory.

This simple view of the wake is shown in figure 4*a* for a 'hovering' propeller, or helicopter rotor. The action of the propeller is replaced by a horizontal Froude actuator disc of area $A_0 = \pi L^2$, where L is the length of the propeller blades. The pressure exerted by the disc on the air is assumed to be constant over its area and steady with time. This causes a downward acceleration of the air that continues for some distance below the disc because of the high pressure in the jet. The jet pressure gradually returns to atmospheric far below the disc, and the air velocity then remains constant. Using Bernoulli's equation, the theory shows that the vertical velocity w finally attained in the 'far' wake is twice the induced velocity w_0 at the disc: $w = 2\,w_0$. Furthermore, continuity of flow requires that the volume of air passing through the far wake per unit time equals that flowing through the disc, $Aw = A_0\,w_0$, so the far wake area A must be $\frac{1}{2}A_0$. Thus the jet contracts below the disc until the air is accelerated up to its final velocity.

The Rankine–Froude theory may be applied directly to hovering animal flight once a

Downloaded from rstb.royalsocietypublishing.org

suitable actuator 'disc' is defined. Other authors have consistently chosen a circular disc with area $A_0 = \pi R^2$ (e.g. Weis-Fogh 1973; Rayner 1979*a*, *c*), although R. Å. Norberg (1975) did so with some reservations. This is probably taking the propeller analogy too far: the wake dimensions must be influenced by the stroke angle Φ and the stroke plane angle β. It seems much more appropriate to define A_0 as the area over which the wings actually impart downward momentum to the air, giving $A_0 = \Phi R^2 \cos\beta$ as for the pulsed actuator disc. The *shape* of the Froude 'disc' is irrelevant to the theory, so the animal's disc can be pictured as the two pie-shaped sections shown in figure 4*b*. This should be a good representation of the wing action and indicates that two jets are formed below the animal. The total area A of both jets in the far wake is still $\frac{1}{2}A_0$, though, and the velocity w in each jet is $2w_0$. Although figure 4*b* conveniently shows the cross-sectional shape of the far wake to be the same as the disc, this cannot be concluded from the theory; indeed, there are good reasons to suspect that the jet under each wing will change shape while retaining the same area.

The momentum equation for fluids may be applied to the far wake, and it gives the force F required to generate a steady flow of velocity w over an area A as

$$F = \rho w^2 A. \tag{12}$$

This simply equates the force F to the rate of change of momentum of the jet, which is equal to the product of mass flow, ρwA, and velocity w. Equation (12) may be rewritten in terms of w_0 and A_0 using the relations above and, when equated to the weight of the animal, the unknown induced velocity w_0 can then be found:

$$w_0^2 = mg/2\rho A_0 = p_d/2\rho. \tag{13}$$

The useful parameter p_d $(= mg/A_0)$ is the pressure exerted by the disc on the air – the *disc loading*.

The power required to create the jet is equal to the work per unit time done by the disc on the air, Fw_0. Because this work is responsible for the kinetic energy that appears in the steady jet far below the animal, the power may also be derived from the kinetic energy flux in the far wake, $\frac{1}{2} \times$ mass flow $\times$ (velocity)^2. This power is equal to the induced power of the wings, giving

$$P_{ind} = Fw_0 = \tfrac{1}{2}\rho w^3 A. \tag{14}$$

The specific induced power P^*_{ind} is conventionally used in the literature and is equal to the induced power per unit weight supported. From equations (13) and (14),

$$P^*_{ind} = w_0 = \sqrt{(p_d/2\rho)} = P^*_{RF}, \tag{15}$$

which is the final form of the theory. The Rankine–Froude estimate of P^*_{ind} will prove especially useful in the derivation of more advanced models, and so is denoted by P^*_{RF}.

The Rankine–Froude analysis of the wake is elegant in its simplicity; only one parameter, the disc loading p_d, is needed to estimate the induced velocity and power of the wings. For a given weight support this parameter is entirely governed by the area of the disc, so A_0 must be carefully defined. Consider an animal hovering with a horizontal stroke plane and a typical stroke angle Φ of 2 rads, for example: the induced power estimated from the conventional value of $A_0 (= \pi R^2)$ would be 20% below that from my definition of $A_0 (= \Phi R^2 \cos\beta)$. This is a substantial discrepancy, and the results for an inclined stroke plane with smaller Φ differ even more. Apart from this problem about the disc area, the model is well-suited for the analysis

Downloaded from rstb.royalsocietypublishing.org

of hovering animal flight: it is easy to apply and gives the absolute minimum value of the induced power.

3.2. *The simplest vortex theory*

A momentum theory considers only the initial and final states of the air acted upon, and hence does not require any knowledge of the aerodynamic mechanism used by a propeller or flying animal. Indeed, the operating mechanism is treated as a black box, the Froude disc, which somehow exerts a pressure over a limited area in the air. A vortex theory of hovering, though, is derived from an understanding of the mechanism itself. The pressure applied to the air by the blades (or wings) can be attributed to the circulation around them, which also causes free vortices to be shed into the wake. Because the wake motion is determined by the induced velocity field of these shed vortices, the pressure exerted by the blades can be directly related to the induced velocity and power. It is very difficult in general to calculate the induced velocities of a vortex wake, however, and modern methods are often forced to rely heavily on numerical techniques that are not altogether satisfactory. Fortunately, some physical approximations can be invoked for most hovering propellers and animals, leading to vortex theories as simple as the momentum theories.

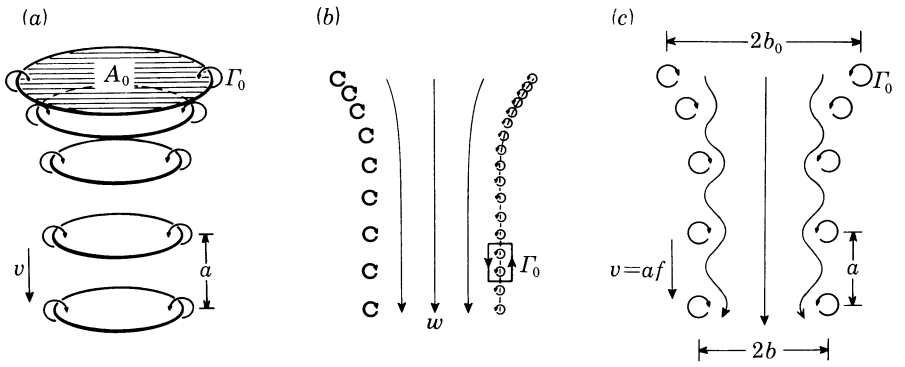

FIGURE 5. (*a*) The vortex wake of a pulsed circular Froude disc may be represented by an axial chain of circular vortex rings. (*b*) If the axial separation a is negligible, as assumed in the simple vortex theory, then the discontinuous vortex boundary can be approximated by a continuous vortex sheet. (*c*) For larger separations, the wake velocities show periodic variations that increase the specific induced power.

As discussed in §2.4, the vorticity shed from the wings can be modelled by the horizontal vortex sheets produced by a pulsed actuator disc. Vorticity will be continuously distributed over each sheet in general, but the complexity of the distribution vanishes for one special case: if the circulation is constant along the wings while each sheet is generated, then the shed vorticity consists of a single vortex line around the perimeter of the sheet. Thus the circulation Γ is constant over the pulsed disc and will be denoted by Γ_0 for this special case; Γ_0 must be equal to the maximum circulation Γ_{max}, which is $p_d/\rho f$ according to equation (11) and the definitions of p_d and $\hat{I}$. For a circular disc, as shown in figure 5*a*, each pulse therefore creates a single circular vortex ring of area A_0 and circulation Γ_0. The rings move downwards under their induced velocity field, forming an axial chain of vortex rings in the wake. The rings will be close together when the frequency f of impulses is very high, and as f approaches infinity they will merge into a continuous cylindrical vortex sheet moving downwards from the disc perimeter. To construct a simple vortex theory of hovering, we need only assume that the frequency is high

Downloaded from rstb.royalsocietypublishing.org

enough for the discrete rings to be approximated by such a continuous sheet. This approximation is illustrated in figure 5*b*, which shows a vertical section through the wake: the vorticity concentrated in each ring on the left-hand boundary is considered to be distributed uniformly over the small axial distance between the rings, and results in the vortex sheet of the right-hand boundary. Circulation must be conserved when redistributing the vorticity in this manner, so the circulation around a length of the sheet equal to the ring separation must also be Γ_0. Denoting the axial separation of the rings by a in the far wake, the circulation per unit length of the vortex sheet is Γ_0/a far below the disc.

The velocity of a fluid changes abruptly across a vortex sheet, so the smooth cylindrical sheet forms a boundary between the undisturbed air and a steady axial flow in the wake. The velocity difference across a sheet is equal to its circulation per unit length, therefore the velocity w of the far wake with respect to the still air is Γ_0/a. Because of the periodicity of the ring structure the axial separation a must equal v/f, where v is the downward velocity of the rings. Using this relation and the definition of Γ_0, the far wake velocity w can then be written as

$$w = p_d/\rho v. \tag{16}$$

In this simple vortex theory, the ring velocity v can be approximated by the downward velocity of the cylindrical vortex sheet. The inner surface of this sheet moves with the wake velocity w while the outer surface is at rest with the still air, so the sheet travels downwards at an average velocity of $\frac{1}{2}w$. Substituting this value for v, the wake velocity is finally given by

$$w^2 = 2f\Gamma_0 = 2p_d/\rho. \tag{17}$$

It should be apparent that we have just derived the Rankine–Froude axial momentum jet from a different approach, that of the vorticity shed from the pulsed disc. This disc is a pulsed Froude disc, in fact, applying a uniform pressure impulse $\rho\Gamma_0$ over its area. Thus the simplest vortex theory of hovering, with constant circulation across the disc and a high frequency of impulses, provides the same wake model as the axial momentum theory. The analysis of this wake by either approach must yield the same answers, of course, and equation (17) agrees with the wake velocity already presented in the Rankine–Froude theory. Although illustrated here for a circular pulsed Froude disc, the simple vortex approach is equally applicable to a hovering animal. Indeed, this approach provides very strong support for my definition of the disc area A_0 as $\Phi R^2 \cos\beta$. Because vorticity can be created only at the interface between the wings and the air, *the vortex boundary of the momentum jet must be restricted to the area actually swept by the beating wings*.

3.3. *A differential momentum–vortex theory*

The operation of the propeller blades, or animal wings, has been grossly simplified in the two theories just presented. It has been assumed that the aerodynamic mechanism applies a *continuous*, *uniform* pressure to the air, and these restrictions must be removed to construct more accurate models of the wake. This section takes one step towards a more general theory by considering the wake produced by a *modified* Froude disc that exerts a steady, but non-uniform pressure over its area. The effects of periodic pressure pulses will be reserved for the following section.

Downloaded from rstb.royalsocietypublishing.org

3.3.1. *The momentum ingredient*

The steady wake produced by a modified Froude disc is analysed in propeller theory using a differential form of the momentum equations. Because of axial symmetry, the vertical force is a function only of radial position for a hovering propeller. Thus the modified Froude disc can be regarded as a set of concentric annuli, or rings, each of which exerts a characteristic pressure. The air passing through a particular annulus forms a hollow cylinder below the disc, as shown in figure 4*a*, and the wake corresponds to the nested cylinders from all of the annuli. In the differential momentum theory of propellers, it is assumed that the momentum equations used in the Rankine–Froude theory can be applied independently to the steady cylindrical flow of each annulus. If w is the velocity of this flow over the cross-sectional area $\mathrm{d}A$ of the hollow cylinder in the far wake, then the force $\mathrm{d}F$ and induced power $\mathrm{d}P_{\mathrm{ind}}$ required from the disc annulus are given by

$$\mathrm{d}F = \rho w^2 \,\mathrm{d}A, \tag{18}$$

$$\mathrm{d}P_{\mathrm{ind}} = \tfrac{1}{2}\rho w^3 \,\mathrm{d}A. \tag{19}$$

The area $\mathrm{d}A_0$ and induced velocity w_0 of the disc annulus are related to the far wake parameters in the same way as the Rankine–Froude theory: $w = 2w_0$, and $\mathrm{d}A = \frac{1}{2}\mathrm{d}A_0$.

The axial symmetry of the propeller disc is absent for a hovering animal, so it is more appropriate in that case to consider a *streamtube* passing through the disc into the far wake (figure 4*b*). The equations of force $\mathrm{d}F$ and induced power $\mathrm{d}P_{\mathrm{ind}}$ for a streamtube are the same as for a propeller annulus, except that $\mathrm{d}A$ and $\mathrm{d}A_0$ now refer to the cross-sectional areas of the streamtube.

Although this differential form of the axial momentum theory is widely used for propellers, its validity has not been established. The proper momentum equations for fluids are, in fact, derived as *integral* equations: the total force of a steady jet is given by the integral of the momentum flux across its area, and the total power is equal to the integral of the kinetic energy flux. The assumption that these equations are valid in *differential* form implies that the cylindrical flow from each annulus is not influenced by adjacent cylinders. Many authors have discussed this problem without drawing firm conclusions, but the general consensus is that the assumption should be a reasonable approximation to the real events.

3.3.2. *The vortex ingredient*

The differential momentum theory succeeds in relating the induced power and velocity to the local pressure exerted by the disc, but it can go no further. Precisely because the momentum approach ignores the details of the aerodynamic mechanism, it cannot be used to determine the actual pressure distribution. In propeller theory this information is usually provided by a force coefficient blade-element analysis, but this method is not very suitable for our unsteady aerodynamic mechanisms. It will prove more useful to employ a vortex approach instead, as done in the more sophisticated propeller theories. Those theories generally use a lifting-line vortex theory to specify the pressure distribution, but the generalized pulsed actuator disc model is also quite suitable.

The vertical force $\mathrm{d}F$ exerted on a small area $\mathrm{d}A_0$ of the modified Froude disc must equal the mean force locally applied by the pulsed actuator disc. The vertical force impulse $\mathrm{d}I_0$ over this area is $\rho\Gamma\,\mathrm{d}A_0$, so the mean force is just $\rho f\Gamma\,\mathrm{d}A_0$.

PHILOSOPHICAL TRANSACTIONS OF THE ROYAL SOCIETY B BIOLOGICAL SCIENCES
PHILOSOPHICAL TRANSACTIONS OF THE ROYAL SOCIETY B BIOLOGICAL SCIENCES

Downloaded from rstb.royalsocietypublishing.org

Writing

$$dF = 2\rho w_0^2 \, dA_0 = \rho f \Gamma \, dA_0, \tag{20}$$

the induced velocity w_0 of the streamtube, or annulus, can then be expressed in terms of the local disc circulation. Γ is equal to $\hat{\Gamma}\Gamma_{\max}$, though, and equation (11) shows that

$$\Gamma_{\max} = p_d/\rho f \hat{I}. \tag{21}$$

The local induced velocity can therefore be written as

$$w_0 = \left[\frac{p_d}{2\rho}\frac{\hat{\Gamma}}{\hat{I}}\right]^{\frac{1}{2}} = w_{0,\,\mathrm{RF}}\sqrt{(\hat{\Gamma}/\hat{I})}, \tag{22}$$

where $w_{0,\,\mathrm{RF}}$ is the induced velocity calculated from the Rankine–Froude theory. Remembering that $\hat{I}$ is equivalent to the mean value of $\hat{\Gamma}$ over the disc area, w_0 is also given as

$$w_0 = w_{0,\,\mathrm{RF}}\sqrt{(\hat{\Gamma}/\bar{\hat{\Gamma}})}. \tag{23}$$

Thus the local induced velocity is simply equal to the Rankine–Froude value multiplied by the square root of the local circulation divided by the mean circulation.

The total induced power expended by the wings is obtained by integrating dP_{ind} over the disc area. Using equation (19) and the relations between the far wake and disc parameters, the total induced power P_{ind} is given by

$$P_{\mathrm{ind}} = 2\rho \iint_{A_0} w_0^3 \, dA_0. \tag{24}$$

The induced velocity from equation (22) can be substituted into this integral and, with the help of the non-dimensional parameters of wing position, the specific induced power for hovering animals can be written as

$$P^*_{\mathrm{ind}} = P^*_{\mathrm{RF}}\frac{1}{\bar{\hat{I}}^{\frac{3}{2}}}\int_{-1}^{1}\int_{0}^{1}\hat{\Gamma}^{\frac{3}{2}}\hat{r}\,d\hat{r}\,d\hat{\phi}, \tag{25}$$

where P^*_{RF} is the Rankine–Froude estimate. The integral in equation (25) is equal to the mean value of $\hat{\Gamma}^{\frac{3}{2}}$ over the disc area, so the specific induced power can also be expressed by

$$P^*_{\mathrm{ind}} = P^*_{\mathrm{RF}}[\overline{\hat{\Gamma}^{\frac{3}{2}}}/\bar{\hat{\Gamma}}^{\frac{3}{2}}]. \tag{26}$$

Like the induced velocity, P^*_{ind} is equal to the Rankine–Froude estimate multiplied by a factor that depends only on the normalized distribution of circulation over the disc. The bracketed ratio in equation (26) must always be greater than or equal to 1, so the specific induced power for a differential disc can never be less than the Rankine–Froude value. The ratio will equal 1 only if $\hat{\Gamma}$ is constant and therefore equal to 1 over the disc: for that special case the applied pressure is the same for all streamtubes, so the differential disc is equivalent to the Froude disc. Even when $\hat{\Gamma}$ is not constant, though, the ratio is unlikely to be much greater than 1. I have previously calculated P^*_{ind} for some reasonable circulation profiles, and they were only about 8% above the Rankine–Froude estimate (Ellington 1978). Values for the insects in paper III will be given later in paper VI, but they are much the same.

Whether this theory should be called a 'differential momentum theory' or a 'vortex theory' is largely a matter of personal preference. Both names are used in propeller theory, and I have included both in the title of this section for reasons of diplomacy. By combining the two approaches, the induced velocity and power have been related to the circulation responsible for the vertical aerodynamic force. This is the goal of a vortex theory, of course, so that name

PHILOSOPHICAL TRANSACTIONS OF THE ROYAL SOCIETY B BIOLOGICAL SCIENCES
PHILOSOPHICAL TRANSACTIONS OF THE ROYAL SOCIETY B BIOLOGICAL SCIENCES

Downloaded from rstb.royalsocietypublishing.org

may be somewhat more appropriate. Furthermore, the momentum approach is not a necessary part of the theory, because it could be replaced in principle by a vortex analysis similar to the simple vortex theory. We would then consider a vertical vortex sheet separating adjacent annuli from a propeller disc, giving a vortex wake model of co-axial cylindrical vortex sheets. In the same manner, the adjacent streamtubes from an animal disc would be separated by a vortex sheet, indicating a honeycomb-like vortex structure for the wake. The axial velocity difference between adjacent annuli, or streamtubes, is given by the circulation per unit length of the separating vortex sheet, so the absolute axial velocity could be obtained by integrating in from the wake boundary. The differential momentum theory must give the same results, however, and it is certainly much more convenient to use.

3.4. *A theory of wake periodicity*

In this section, the wake model is further improved by investigating the effects of a periodic application of pressure to the air. An introduction to the subject has already been provided by the simple vortex theory, which considered the wake produced by a pulsed circular Froude disc. The uniform pressure distribution over this disc during a pulse results in a single vortex ring around its perimeter, and the wake consists of an axial chain of such rings. A vertical section of the wake is drawn in figure 5*c*, showing that the wake velocities are not steady when the vortex boundary is discontinuous: the jet tends to flow outwards and slow down between adjacent vortex rings, and it contracts and speeds up inside each ring. This produces a pulsating, quasi-steady, periodic jet with horizontal velocity components that must increase in magnitude with large axial separations of the rings.

These horizontal velocity components require energy, of course, but they do not contribute to the axial momentum flux supporting the animal's weight. Thus they represent an energy loss, and the induced power for such a periodic wake must be greater than a steady jet generating the same force. The increased power requirement is related to the *tip losses* of propeller theory, a problem addressed by Prandtl (1919), Goldstein (1929) and many others: see Bramwell (1976) for a review. For various reasons their analyses are not directly applicable to hovering animal flight, so I have developed a new theory that once again uses the powerful combination of momentum and vortex approaches.

The theory could, in principle, be developed along two lines. With the Rankine–Froude theory corrected for a non-uniform pressure distribution over the disc, we could now analyse the effects of periodicity on the differential momentum–vortex model. Alternatively, the influence of periodicity could be studied in isolation by considering the wake of a pulsed Froude disc. I have chosen the second method because its separate treatment is more attractive conceptually, allowing the two major deficiencies of the Rankine–Froude theory to be corrected independently by appropriate modifications to the basic Froude disc. This sense of continuity is conspicuously absent in propeller theory, which discards the Rankine–Froude model when investigating tip-losses.

3.4.1. *The quasi-steady momentum jet*

We begin by applying the momentum equations to the periodic wake of a pulsed Froude disc. As in the Rankine–Froude theory, it is assumed that the mean pressure in the far wake is the same as the surrounding air, and that a wake boundary does exist. The second assumption may seem questionable since the vortex boundary is discontinuous, but the classical analysis

Downloaded from rstb.royalsocietypublishing.org

of a two dimensional Kármán vortex street shows that a time-averaged mean boundary certainly exists for quasi-steady periodic wakes. In this theory it is only assumed that some instantaneous boundary *could* be defined which yields the mean boundary on average, but details of the boundary will not be required. The far wake parameters are all periodic functions of time: the cross-sectional area A, the vertical velocity component w, and the magnitude of the net velocity vector q, which includes both vertical and horizontal velocity components. The momentum equations can be used to determine the mean vertical force and mean induced power of the periodic, quasi-steady jet if both sides of the equations are assigned their mean values (see Prandtl & Tietjens 1957*a*; Mises 1959). Thus the mean force and power are given by the mean values of the momentum and energy fluxes:

$$\bar{F} = \rho\overline{Aw^2}, \tag{27}$$

$$\overline{P_{\text{ind}}} = \tfrac{1}{2}\rho\overline{Awq^2}, \tag{28}$$

where bars indicate time averages, and ρ is taken as constant because the air is effectively incompressible. In the limit as the axial ring separation vanishes, the net velocity q approaches the vertical component w, all wake parameters become steady with time, and these equations then reduce to those of the Rankine–Froude theory.

Continuity of flow requires Aw to be constant, if it is assumed that a wake boundary exists, so this product can be removed from the averaged quantities. If we restrict the analysis to wakes with a *slight periodicity*, the horizontal component will be small and q may be approximated by w. The mean specific induced power from equations (27) and (28) is then

$$\overline{P^*_{\text{ind}}} = \overline{P_{\text{ind}}}/\bar{F} = \overline{w^2}/2\bar{w}. \tag{29}$$

Siekmann (1963) applied the unsteady Bernoulli equation to the periodic momentum jet generated by a pulsed Froude disc, and he derived another expression for the mean force as

$$\bar{F} = \tfrac{1}{2}\rho A_0\,\overline{w^2}, \tag{30}$$

where A_0 is the area of the disc. The periodic jet must produce the same mean force as the steady Rankine–Froude jet for weight support, so equation (30) must also equal $\frac{1}{2}\rho A_0\, w^2_{\text{RF}}$, where w_{RF} is the steady axial velocity in the far wake of the Rankine–Froude model. This shows that $\overline{w^2}$ is equal to w^2_{RF} and, remembering that $w_{0,\,\text{RF}} = \frac{1}{2}w_{\text{RF}}$, equation (29) can be reduced to

$$\overline{P^*_{\text{ind}}} = w_{0,\,\text{RF}}\, w_{\text{RF}}/\bar{w} = P^*_{\text{RF}}\, w_{\text{RF}}/\bar{w} = kP^*_{\text{RF}}. \tag{31}$$

Thus the specific induced power of a quasi-steady jet with small periodicity can be written as a factor k times the steady Rankine–Froude value, where k is the ratio in the far wake of the Rankine–Froude velocity to the mean velocity of the periodic wake. P^*_{RF} is the theoretical minimum for the specific induced power, so k must be greater than unity for a periodic wake, and $\bar{w}$ is therefore less than w_{RF}.

3.4.2. *The vortex wake*

Although the mean wake velocity $\bar{w}$ cannot be determined from the momentum approach, it is readily calculated from the type of vortex analysis used for a Kármán vortex street. As in the simple vortex theory, the circulation Γ_0 of each ring from the pulsed Froude disc is equal to $\Gamma_{\text{max}}(= p_{\text{d}}/\rho f)$, the downward velocity of the rings in the far wake is v, and the axial ring separation there is a $(= v/f)$. Each vortex ring moves steadily through the distance a along

Downloaded from rstb.royalsocietypublishing.org

the mean wake boundary during the cycle period $1/f$, which is equivalent in a time-averaged view to a uniform distribution of the ring vorticity along the length a. The circulation per unit length of the mean boundary is therefore Γ_0/a, and this must equal the mean velocity difference across the boundary. Thus the mean wake velocity can be written as

$$\bar{w} = p_d/\rho v, \tag{32}$$

which is the time-averaged version of equation (16) from the simple vortex theory.

The specific induced power is now a function of only one unknown, the axial ring velocity v, which was the final important parameter of the simple vortex theory as well. However, the mean velocity of a continuous vortex sheet cannot be used again to estimate v beause this would remove the effects of periodicity from the model. The ring velocity must be calculated directly instead, and it is much easier to do this if we assume that the rings are circular: the errors possibly introduced by this assumption will be discussed later. Thus the wake shall be idealized as an axial chain of circular vortex rings which are created by a pulsed circular Froude disc. The initial ring radius b_0 at the disc is $\sqrt{(A_0/\pi)}$, but the rings contract as they move down the wake. Far below the disc, the wake is characterized by the ring radius b, the axial separation a, and the axial ring velocity v (figure 5*c*). The circulation of each ring cannot change with time, so it is always equal to the initial value Γ_0.

Levy & Forsdyke (1927) have investigated the velocity at which a circular vortex ring moves along the axis of an infinite chain of identical rings, and their results may be applied to the far wake. The velocity v of each ring has two components: (i) the induced velocity from other rings in the chain, and (ii) the self-induced velocity of the vortex ring under consideration. It is convenient to reduce the equations of Levy & Forsdyke to the following expression,

$$v = \frac{\Gamma_0}{b}[K(a/b) + C]. \tag{33}$$

K is a function describing the influence of the rest of the chain on the velocity, and it is only dependent on the *spacing ratio* a/b of the rings. K is readily calculated numerically from the equations of Levy & Forsdyke, and is shown by the curve in figure 6.

The vorticity responsible for the circulation of a vortex ring is confined to a *core* region, about which the irrotational flow recirculates. The constant C, which represents the contribution of the self-induced velocity to the total axial ring velocity v, is determined only by the distribution of vorticity in the core, but we have no information concerning that distribution. The action of viscosity within the core of a vortex ring often tends to produce a circular core that rotates like a solid cylinder, however, and this form can be used for an initial estimate of C. The radius ϵ of the circular cross-section of such a core is usually expressed non-dimensionally by the core-to-ring radius ϵ/b. C can then be derived from the equations of Levy & Forsdyke as

$$C = \frac{1}{4\pi}\left[\ln\left[\frac{8b}{\epsilon}\right] - \tfrac{1}{4}\right], \tag{34}$$

where the constant $\frac{1}{4}$ reflects the choice of a circular core with constant rotation. Reasonable values of ϵ/b may be expected in the range of 0.05 to 0.25 for this theory; larger cores may begin to overlap with those of adjacent rings under our restriction of small periodicity. The volume of the core must remain constant as the rings contract alont the wake, so if ϵ_0 and ϵ denote the initial value at the disc and the value in the far wake, respectively, they are related by $b\epsilon^2 = b_0\epsilon_0^2$.

PHILOSOPHICAL TRANSACTIONS OF THE ROYAL SOCIETY B BIOLOGICAL SCIENCES
PHILOSOPHICAL TRANSACTIONS OF THE ROYAL SOCIETY B BIOLOGICAL SCIENCES

Downloaded from rstb.royalsocietypublishing.org

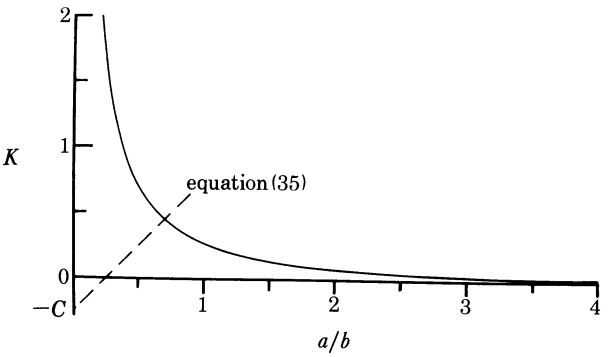

FIGURE 6. Values of K, representing the axial velocity of an individual vortex ring owing to an infinite chain of rings, plotted against the spacing ratio a/b. The linear relation of equation (35) is shown by the dashed line.

The wake boundary must converge on the Rankine–Froude geometry when the axial separation vanishes, so the wake area A must approach $\frac{1}{2}A_0$ in that limit. Because the theory has already been restricted to wakes with small periodicity, A can be approximated by that value and b is then equal to $\sqrt{(A_0/2\pi)}$. This result and the definition of Γ_0 can now be substituted into equation (33). The axial ring velocity must satisfy the requirement of vorticity flux in the wake as well as the Levy–Forsdyke relation, so the right-hand side of equation (33) can be equated to af to produce

$$K(a/b) = \frac{1}{s^2}\frac{a}{b} - C, \tag{35}$$

where

$$s^2 = 2\pi p_d/\rho A_0 f^2. \tag{36}$$

Thus considerations of vorticity flux demand a linear relation between K and a/b, as shown in figure 6, that depends only on the *spacing parameter* s and the assumed value of C. The intersection of this line with the curve from Levy & Forsdyke yields the only value of a/b consistent with both the axial velocity of the chain and the vorticity flux required to support a given weight. Thus s defines a unique value of the spacing ratio a/b for a given self-induced velocity, and in doing so it determines the velocity v of the rings. From previous definitions, s is basically proportional to the Rankine–Froude induced velocity $w_{0,\,\mathrm{RF}}$ divided by the mean wing tip velocity $\overline{U_t}$ (paper III), but it also accounts for the influence of the inclination of the stroke plane on the wake geometry and the relation between impulse and wingbeat frequencies.

The spacing ratio a/b is plotted against the spacing parameter s in figure 7*a* for C equal to 0.384, 0.297 and 0.256. (These values were calculated from equation (34) for ϵ/b equal to 0.05, 0.15 and 0.25 respectively, thus covering the range which might be expected.) The three curves are quite similar for small s; this indicates that the velocity of a particular ring is primarily governed by the induced velocity from the other rings when they are closely stacked. The curves appear to converge on the origin, which is the expected Rankine–Froude limit for vanishing axial separation as the frequency becomes infinite. For larger values of s and a/b, however, the curves increasingly diverge. This corresponds to the self-induced velocity of each vortex ring dominating its axial velocity when the rings are well-separated, and the choice of C then has a strong influence. The maximum value of the spacing parameter s found for hovering animals is 4 (Ellington 1980).

Downloaded from rstb.royalsocietypublishing.org

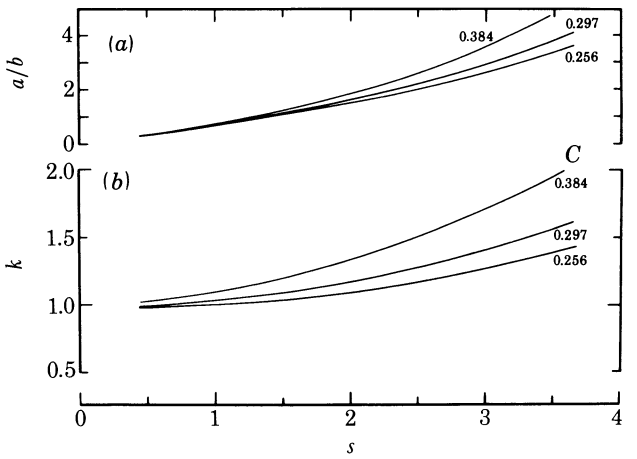

FIGURE 7. (*a*) The spacing ratio a/b plotted against the spacing parameter s for three values of C. (*b*) A similar graph of the induced power factor k.

3.4.3. *Induced power*

By substituting equation (35) and the definitions of Γ_0 and b into equation (33), an expression for v is obtained that can be used to determine the mean wake velocity of equation (32). By combining this with the definition of w_{RF}, we can finally derive an equation for the induced power factor k:

$$k = \frac{\sqrt{2}}{s}\frac{a}{b}. \tag{37}$$

The results of figure 7*a* are then used to express a/b in terms of the spacing parameter s and the three assumed values of C, giving the factor k as a function of s in figure 7*b* for those values. All three curves converge on a value of k near unity as s approaches zero, the limit of the Rankine–Froude steady jet. Extrapolation yields $k(0)$ equal to 1.01, 0.99, and 0.98 for C equal to 0.384; 0.297 and 0.256 respectively. The difference between these values and unity is within the error of the approximations but shows a systematic variation with C. The curves increasingly diverge as s increases, but this is again because of the dominance of the self-induced ring velocity.

We now turn to the selection of an appropriate estimate for the constant C in the vortex ring model. The specific induced power for the periodic wake must always be greater than the Rankine–Froude value for a steady jet, and it should converge on that value in the limit of vanishing periodicity. The results for the two smaller estimates of C (0.256 and 0.297) yield k less than unity as s approaches zero, which clearly violates these momentum considerations. The value of 0.384 is therefore selected as the most suitable for use in the ring model: it provides close agreement with the Rankine–Froude theory and does not contradict the theoretical minimum specific induced power. This value of C corresponds to a circular cored vortex ring with ϵ/b equal to 0.05, which is perhaps smaller than might be expected. There is little justification in assuming that the core is actually circular, however; details of the shape and vorticity distribution of the core are lacking, and the simple circular core was chosen only as a convenient means of estimating C. Indeed, physical intuition suggests that at small s the core cross-section should be somewhat lens-shaped with its major axis parallel to the wake axis.

PHILOSOPHICAL TRANSACTIONS OF THE ROYAL SOCIETY B BIOLOGICAL SCIENCES
PHILOSOPHICAL TRANSACTIONS OF THE ROYAL SOCIETY B BIOLOGICAL SCIENCES

Downloaded from rstb.royalsocietypublishing.org

The results for $k(s)$ are very nearly quadratic, and may be described for C equal to 0.384 by

$$k(s) = 0.079\,s^2 + 1, \tag{38}$$

where $k(0)$ is set equal to unity for agreement with the Rankine–Froude limit. If the intercept of 1.01 from figure 7*b* is used instead, then equation (38) fits the curve to better than 1% over most of the range of s. Equations (37) and (38) may be combined to give

$$\frac{a}{b} = 0.056\,s^3 + 0.71\,s, \tag{39}$$

thus expressing the spacing ratio a/b solely in terms of the spacing parameter s as well.

3.4.4. *Induced velocity*

The induced velocity can also be estimated for the pulsed Froude disc using the small periodicity analysis. The mean induced power of the periodic wake must equal the mean rate at which work is done by the disc, $\overline{F w_0}$. The impulsive force acts only for a brief time τ during the period $1/f$, though, and it is otherwise zero. By considering a time τ so short that the force and induced velocity are effectively constant during the impulse, the mean power can then be written as

$$\overline{P_{\mathrm{ind}}} = F_{\mathrm{i}}\, w_{0,\mathrm{i}}\, \tau f, \tag{40}$$

where the subscript i denotes values for the impulse. The impulsive force must equal $\bar{F}/\tau f$, however, so the mean specific induced power is simply $w_{0,\mathrm{i}}$. Comparing this to the periodic approximation of equation (31) shows that

$$w_{0,\mathrm{i}} = k w_{0,\mathrm{RF}}. \tag{41}$$

Thus the increased $\overline{P^*_{\mathrm{ind}}}$ of the periodic jet indicates that the induced velocity during application of the impulsive pressure is greater than the Rankine–Froude value by the same factor k. This enhancement of the induced velocity is to be expected from physical reasoning as well: the impulsive pressure creates a vortex ring as it accelerates the air downwards, and the velocities of a periodic wake are greatest inside the bounding vortex rings.

3.5. *Total induced power and velocity*

The two modifications to the Rankine–Froude axial momentum theory must now be combined to arrive at the total specific induced power requirement of hovering. The first modification, the differential Froude disc, provides a *spatial* correction factor for a non-uniform disc pressure and circulation. This correction depends on the circulation profile, but it is unlikely to be greater than about 10% of P^*_{RF} for reasonable profiles (Ellington 1978). The second modification, derived from the quasi-steady jet produced by a pulsed Froude disc, gives a *temporal* correction factor for the periodic application of the disc pressure. This correction is a function of the spacing parameter s and is also small in general, less than about 10% for values of s corresponding to small wake periodicities (Ellington 1980). Because these two corrections are quite small, they may be treated as effectively independent perturbations of the Rankine–Froude model: one introduces spatial variations in wake velocities, the other considers temporal variations, so any interactions will be of second order and probably negligible. Thus we can

Downloaded from rstb.royalsocietypublishing.org

add the correction factors linearly and express the *total* mean specific induced power requirement as

$$\overline{P^*_{\mathrm{ind}}} = P^*_{\mathrm{RF}}(1+\sigma+\tau), \tag{42}$$

where the *spatial correction factor* σ and the *temporal correction factor* τ are defined by

$$\sigma = \frac{1}{\hat{I}^{\frac{3}{2}}}\int_{-1}^{1}\int_{0}^{1}\hat{\Gamma}^{\frac{3}{2}}\hat{r}\,\mathrm{d}\hat{r}\,\mathrm{d}\hat{\phi} - 1 = \overline{\hat{\Gamma}^{\frac{3}{2}}}/\overline{\hat{\Gamma}^{\frac{3}{2}}} - 1, \tag{43}$$

$$\tau = k - 1 = 0.079\,s^2, \tag{44}$$

according to equations (25), (26), (31) and (38).

The total induced velocity can also be estimated from linear addition of the spatial and temporal corrections when the assumptions of the theory are satisfied. Using equations (15), (22) and (41), the *local* induced velocity w_0 during the impulse can be written as

$$w_0 = P^*_{\mathrm{RF}}[\tau + \sqrt{(\hat{\Gamma}/\hat{I})}]. \tag{45}$$

The induced velocity is a periodic function of time, and equation (45) is valid only during the application of the impulse; thus it provides an estimate of the induced velocity experienced locally by the wings as they actually generate lift.

The local orientation of the vortex sheet arising from circulatory lift (§2.1.) is given by vector addition of the local induced velocity and the flapping velocity. This result should be averaged over the entire area swept by the wings to calculate the relative stroke plane angle β_{r}, perhaps weighting the values by the local impulse. These complications are probably unnecessary for our crude planar representation of the helicoidal sheet, however, and a much simpler method should suffice: vector addition of a mean induced velocity to a mean flapping velocity. Spatial variations in the local induced velocity from equation (45) will have no net effect when averaged over the swept area, so the mean induced velocity while the sheet is created can be taken as $P^*_{\mathrm{RF}}(1+\tau)$. The mean wing tip velocity $\overline{U_{\mathrm{t}}} = 2\Phi nR$ was chosen to represent the mean flapping velocity for the definition of the advance ratio J in paper III, and it seems a good choice here for the same reasons. The relative stroke plane angle β_{r} will be different on the half-strokes, and it is given by vector addition as

$$\tan\beta_{\mathrm{r}} = \tan\beta \pm \frac{P^*_{\mathrm{RF}}(1+\tau)}{2\Phi nR\cos\beta}, \tag{46}$$

where the negative sign is used for the downstroke and the positive for the upstroke.

3.6. *Rayner's theory*

Rayner (1979*a*) has also developed a vortex theory of hovering animal flight, by using a numerical analysis to study the evolution of the wake from rest. He begins with the assumption that the vortex sheets produced by the wings roll up immediately into horizontal, circular vortex rings with small circular cores: the ring circulation is equal to the maximum circulation of the sheet, the ring area is found by equating the ring and sheet impulses, but the core radius is an unknown. Starting from rest, Rayner then creates these vortex rings at an appropriate frequency in his numerical model, and calculates their subsequent motion from the total induced velocity field. This frequency is governed by his 'feathering parameter', which is similar to my spacing parameter but does not include the effects of the stroke angle Φ and the stroke plane angle β.

PHILOSOPHICAL TRANSACTIONS OF THE ROYAL SOCIETY B BIOLOGICAL SCIENCES
PHILOSOPHICAL TRANSACTIONS OF THE ROYAL SOCIETY B BIOLOGICAL SCIENCES

Downloaded from rstb.royalsocietypublishing.org

There are clearly strong similarities between Rayner's theory and my treatment of wake periodicity, but this is hardly surprising since small-cored circular vortex rings offer the most obvious tractable representation of the hovering wake. In fact, there are only two basic differences between our wake models. Mine is designed to study the effects of wake periodicity in isolation, so a uniform circulation profile and initial ring area A_0 is assumed, whereas Rayner considers a non-uniform profile with a rolled-up ring area corresponding to $A_0 \hat{I}$. The second difference is that I invoke two approximations for the far wake structure to keep the mathematics simple, if not trivial. I assume that the ring area in the far wake is approximately half the initial area, based on the Rankine–Froude limit of vanishing periodicity, and that the vortex rings are equally spaced along the far wake axis. This reduces the degrees of freedom of the wake model and allows the axial ring separation and hence the spacing ratio a/b to be determined directly from the considerations of vorticity flux and axial ring velocity. Conversely, Rayner avoids any approximations about the far wake structure by developing it from rest in a very lengthy numerical analysis.

3.6.1. *Structure of the wake*

Rayner's results show a fascinating behaviour of the vortex rings as they move downwards in the wake. For large values of the spacing parameter, where ring interaction is negligible, there is a nearly uniform separation of the rings along the wake axis. At low values, however, there is a limited instability of the wake structure: instead of maintaining a uniform axial separation, the rings tend to clump together into large, relatively stable, periodic groups. This periodic break-up of the wake occurs well below the region of ring creation, so it will have a very small influence on the induced velocities there. If the wake is modelled with a uniform axial ring separation it should prove quite adequate for theoretical studies.

It would be misleading to attach too much significance to the interesting wake patterns found by Rayner. These patterns must reflect to some extent the assumptions of perfectly horizontal, circular vortex rings with small circular cores, if indeed they are not an artefact of the assumptions. Rayner discovered that the far wake structure is even dependent on the mathematical function chosen to represent the growth of vorticity in the new rings. If the far wake is sensitive to the growth function of vorticity created uniformly around the perimeter of ideal vortex rings, then we can hardly predict the pattern of wake instabilities for vortex sheets emanating from moving wings and rolling up at an unknown rate.

Rayner's results also show that the wake contracts very rapidly below its origin; this agrees with studies on hovering helicopter rotors (Bramwell 1976). Contraction is effectively complete before the vortex rings move a distance down the wake equal to their initial radius. Rayner finds that the contracted region is very stable with a nearly uniform axial ring spacing, even though the wake structure begins to break up below this region for low values of the spacing parameter. The contraction coefficient, defined as the contracted ring area divided by the initial area, tends to increase with the spacing parameter. This is as expected, because larger axial spacings must decrease the contracting influence of the wake rings on newly created rings. For smaller axial spacings the contraction coefficient appears to approach the Rankine–Froude value of $\frac{1}{2}$, but this convergence is very abrupt at the limit of vanishing periodicity: for values of the spacing parameter applicable to animals, the contraction coefficient is probably greater than $\frac{1}{2}$. Rayner notes that the absolute values of the contraction coefficient are sensitive to his vorticity growth function, unfortunately, so his analysis cannot be used for a reliable

PHILOSOPHICAL TRANSACTIONS OF THE ROYAL SOCIETY B BIOLOGICAL SCIENCES
PHILOSOPHICAL TRANSACTIONS OF THE ROYAL SOCIETY B BIOLOGICAL SCIENCES

Downloaded from rstb.royalsocietypublishing.org

determination of them. However, he shows that the induced power estimate for a given spacing parameter is not influenced by the contraction coefficient, so the low value of $\frac{1}{2}$ assumed by my theory is unlikely to introduce serious errors.

3.6.2. *A comparison of the theories*

The induced power estimates from the two theories will now be examined under a set of conditions that permits an almost exact comparison. Consider a horizontal stroke plane with stroke angle Φ equal to π, and a uniform circulation profile around the wings: this makes Rayner's feathering parameter f equivalent to $s^2/4\pi^2$, and his parameter R' equal to unity. Because Rayner's wake model is numerically evolved from the initial ring specifications, the initial core-to-ring radius ϵ_0/b_0 must be matched in the theories. My value of 0.15 for the core-to-ring radius in the far wake corresponds to ϵ_0/b_0 equal to 0.09, using conservation of core volume as discussed earlier, and this is very close to Rayner's initial value of 0.1. His induced power factor σ is equivalent to my specific induced power factor k under these test conditions, and his results (figure 13 in Rayner 1979*a*) give

$$k = 0.049\,s^2 + 0.97, \tag{47}$$

while my figure 7*b* yields

$$k = 0.047\,s^2 + 0.99. \tag{48}$$

Both equations are determined from the results to within graphical accuracy.

The close agreement between the two theories is very remarkable, especially in view of the quite different methods used to estimate the induced power. Rayner derives it from the energy required to add a new ring to the chain of vortex rings, whereas I use the small periodicity approximations in the equations of a quasi-steady momentum jet. These approximations *should* cause my theory to become increasingly inaccurate with larger s, although it is possible, if unlikely, that the errors from different assumptions cancel out. I previously doubted if my analysis would be of much use for values of s even as large as 4, which is the upper limit for hovering animals (Ellington 1980); equations (47) and (48) still agree to within 3% for s as large as 12, however, which was the highest value Rayner tested. This close agreement at very large values of s is probably fortuitous.

Having established that the two theories are in complete accord under identical test conditions, we proceed to a more general examination of them. Rayner discusses his results for the induced power in relation to two groups: 'normal' hovering, where the stroke plane is horizontal, and 'avian' hovering, where it is inclined. We shall consider the 'normal' hovering group first, which is characterized by low values of the spacing parameter and hence small wake periodicities. Rayner finds that the influence of the initial rolled-up ring *area* is much greater than the effects of wake periodicity for this group, and concludes that a steady momentum jet analysis can be used to determine the induced power. He claims, without proof, that an accurate estimate can be derived from the Rankine–Froude theory simply by changing the area of the Froude disc from πR^2 to the rolled-up ring area ($= A_0 \hat{I}$). Thus the usual theory is presumably corrected for the area actually swept by the wings, and for the circulation profile over the disc.

Both of these refinements implicit in the work of Rayner (1979*a*) had been treated previously (Ellington 1978), though Rayner did not draw comparisons. In fact, his correction for the circulation profile does not agree with the differential momentum–vortex theory, which was first

Downloaded from rstb.royalsocietypublishing.org

presented in that earlier paper and is derived from a widely accepted propeller theory. When my terminology is used, Rayner's corrected induced power can be expressed by

$$P^*_{\mathrm{ind}} = \frac{P^*_{\mathrm{RF}}}{\sqrt{\bar{\hat{\Gamma}}}}, \tag{49}$$

whereas equation (26) of my theory gives

$$P^*_{\mathrm{ind}} = \frac{P^*_{\mathrm{RF}}}{\sqrt{\bar{\hat{\Gamma}}}} \frac{\overline{\hat{\Gamma}^{\frac{3}{2}}}}{\bar{\hat{\Gamma}}}. \tag{50}$$

The extra term in equation (50) reflects the fact that force and power are proportional to different exponents of the velocity in a differential momentum jet. Thus the specific induced power, given by the integral of power divided by the integral of force, must be governed by *two* functions of the circulation profile. Rayner's ring model assumes that the impulse and energy of a vortex sheet do not change with rolling up, so his specific induced power must converge on that of the differential momentum jet in the limit of negligible periodicity. Two parameters in his model *are* functions of the circulation profile: the intial ring area, which is determined by the impulse of the profile, and the core-to-ring radius, which obeys an *unknown* function. Rayner's correction only considers the impulse of the profile, however, and must therefore be incomplete. If used for the circulation profiles in paper VI, his 'correction' can overestimate the specific induced power by up to 30%.

Rayner also applies an impulse modification to his results for 'avian' hovering, where the wake periodicity shows a more pronounced influence on the induced power. Again, I think this procedure is an incorrect interpretation of his numerical results. The dependence of the core radius on the circulation profile cannot be brushed aside, and there is no valid procedure for determining it from a vortex ring model. Indeed, I found it necessary to use the results from an entirely different theory, the momentum theory, to estimate the appropriate value of the core radius for a *single* circulation profile, that produced by a pulsed Froude disc. Rayner did not use the momentum theory to guide the selection of a value for ϵ/b, however, and his three values all yield a specific induced power for the pulsed Froude disc with small periodicity which is *less* than the Rankine–Froude minimum. He suggests that the discrepancy is due to numerical inaccuracies, but this seems improbable since I obtained similar results for large values of ϵ/b using a different method of analysis; as discussed earlier, I think that the assumption of circular cores with uniform vorticity is debatable and liable to underestimate the self-induced velocity of the rings. The need to use a momentum theory in addition to the vortex ring theory may seem ironical, since Rayner (1979*a*, *c*) presents many objections to the former. His objections are sometimes valid in principle for the simple Rankine–Froude theory, but they are quite weak when confronted by the more powerful differential and time-averaged momentum theories.

4. Conclusion

This vortex theory of hovering animal flight complements the discussion of unsteady circulatory lift mechanisms in paper IV. We can only speculate at present how the wing circulation varies with radial position and time, but future experimental and theoretical studies must address this problem. Once the circulation profile during a wingbeat is known, then the mean lift and induced power can be calculated from the vortex theory. However, the only course of investigation praticable now is to evaluate these quantities for *postulated* profiles, as will be done in paper VI.

PHILOSOPHICAL TRANSACTIONS OF THE ROYAL SOCIETY B BIOLOGICAL SCIENCES
PHILOSOPHICAL TRANSACTIONS OF THE ROYAL SOCIETY B BIOLOGICAL SCIENCES

Downloaded from rstb.royalsocietypublishing.org

Although very powerful, a vortex theory is not a panacea for the aerodynamic analysis of animal flight despite suggestions to that effect: 'This novel method of analysis dispenses with the use of lift and induced drag coefficients, both associated with wing circulation and wake vorticity, which have been the main sources of uncertainty in previous calculations' (Rayner 1979*c*). The lift and induced drag coefficients are simply non-dimensional parameters derived from the respective aerodynamic forces, and they can be defined for unsteady motions as well as quasi-steady ones. Any uncertainty about their values only reflects our lack of understanding of the circulatory lift mechanisms, which is perhaps the major problem at present. The vortex theories can hardly alleviate this problem since they are also plagued by it; the uncertainty about circulation profiles is exactly equivalent to that about the force coefficients. Indeed, we have just replaced one set of unknowns with another.

The impulse analysis of the first part of this theory is a very general method for evaluating the mean circulatory lift, and it should prove especially useful for studies on unsteady flight mechanisms. An impulse method was also chosen independently by Maxworthy (1979) and Rayner (1979*a*) for their hovering flight studies, so there appears to be a strong convergence on this technique. The derivation presented here, relating the local impulsive pressure to the circulation around the wings, may provide a helpful physical interpretation of the method for readers unfamiliar with it.

The pulsed actuator disc model of the wing action in hovering offers a unified framework for estimating the mean force, induced velocity and induced power. The approximate description of the wake derived from the pulsed disc is perhaps the most interesting part of the theory, and it is also the best suited for complementary experimental studies. Many authors have investigated the wake of flying animals using hot-wire anemometry or flow visualization techniques (Demoll 1918; Magnan 1934; Magnan *et al.* 1938; Hocking 1953; Wood 1970, 1972; Bennett 1975, 1976; Chance 1975; Ellington 1978, 1980; Kokshaysky 1979). Although these studies are too incomplete for a detailed evaluation of the theory, they offer a tantalizing glimpse of the spatial and temporal variations in wake velocities and the associated vorticity. It must be remembered that the vortex theory is solely concerned with the induced velocities of the wake, however, and that a comparison with measured wake velocities is not straightforward. The induced velocity reflects the downward momentum change of the air corresponding to the lift force, but momentum must also be imparted along the direction of the relative velocity because of the profile drag force. Thus the *net* wake velocities, as determined experimentally, will be composed of nearly vertical induced velocities *and* largely horizontal velocities produced by profile drag. These profile drag velocities are conveniently ignored in a vortex theory of the wake because a separate analysis can be used to calculate the power expenditure associated with them (paper VI).

With careful interpretation, an experimental investigation of the wake structure may evaluate the validity of assumptions and approximations invoked for the vortex theory. Of vital importance is an experimental test of the definition of the disc area A_0, discussed in §3.1. and §3.2.: is it πR^2 or $\Phi R^2 \cos\beta$? This problem is quite tractable for an experimental study of wake velocities using standard techniques. Are the vortex sheets nearly horizontal, thus indicating that the lift is effectively vertical thoughout the cycle? If not, then substantial horizontal components will be imparted to the induced velocities, which will increase the induced power requirement for a given weight support. The horizontal components will cause spreading of the wake as well, disrupting the smooth contraction and simple structure assumed in the theory;

PHILOSOPHICAL TRANSACTIONS OF THE ROYAL SOCIETY B BIOLOGICAL SCIENCES
PHILOSOPHICAL TRANSACTIONS OF THE ROYAL SOCIETY B BIOLOGICAL SCIENCES

Downloaded from rstb.royalsocietypublishing.org

these velocities must be present to some degree, and they are more likely to initiate spreading than the viscous diffusion of wake vorticity discussed by Lighthill (1973). For animals hovering with a horizontal stroke plane, are the individual vortex sheets joined together at either end of the wingbeat by combined stopping and starting vortices, as suggested in paper IV? This would effectively double the axial separation of radial vorticity bounding the wake, further increasing the effect of wake periodicity on the specific induced power. This effect is probably somewhat underestimated already in the periodicity analysis, because the assumption of circular vortex rings reduces the perimeter of the vortex boundary and therefore decreases its influence on the jet.

Even if future experimental studies show that the theoretical model is a crude approximation of the wake, the specific induced power is unlikely to be affected seriously. The classic results from propeller theories indicate that the specific induced power of a momentum jet is remarkably insensitive to the quality of approximations used in its analysis. Estimates of $\overline{P^*_{\mathrm{ind}}}$, including the spatial and temporal corrections, will be presented in paper VI. For animals that hover with a horizontal stroke plane $\overline{P^*_{\mathrm{ind}}}$ is usually greater than the Rankine–Froude estimate by less than 20%, which compares well with hovering helicopters (Bramwell 1976). Thus the corrections from the second part of the theory, although providing a more satisfying physical and conceptual description of the wake, actually yield small benefits over the elegantly simple Rankine–Froude theory. The specific induced power for insects hovering with an inclined stroke plane is about 60% greater than the Rankine–Froude estimate, however, because of the enhanced wake periodicity. Further refinements of the theoretical model may somewhat improve the accuracy of the estimates for them.

I thank Dr D. R. Moore for a useful computing trick, Dr K. E. Machin for discussions and comments on the manuscript, and the Winston Churchill Foundation and the Science and Engineering Research Council for financial support.

References

Bennett, L. 1975 Insect aerodynamics near hovering. In *Swimming and flying in Nature* (ed. T. Y. Wu, C. J. Brokaw & C. Brennen), vol. 2, pp. 815–828. New York: Plenum Press.

Bennett, L. 1976 Induced airflow created by large hovering beetles. *Ann. ent. Soc. Am.* **69**, 985–990.

Betteridge, D. S. & Archer, R. D. 1974 A study of the mechanics of flapping wings. *Aeronaut. Q.* **25**, 129.

Bramwell, A. R. S. 1976 *Helicopter dynamics*. London: Edward Arnold.

Chance, M. A. C. 1975 Air flow and the flight of a noctuid moth. In *Swimming and flying in Nature* (ed. T. Y. Wu, C. J. Brokaw & C. Brennen), vol. 2, pp. 829–843. New York: Plenum Press.

Cone, C. D. 1968 The aerodynamics of flapping bird flight. *Spec. scient. Rep. Va. Inst. mar. Sci.* No. 52.

Demoll, R. 1918 *Der Flug der Insekten und der Vögel*. Jena: Fischer.

Ellington, C. P. 1978 The aerodynamics of normal hovering flight: three approaches. In *Comparative physiology – water, ions and fluid mechanics* (ed. K. Schmidt-Nielsen, L. Bolis & S. H. P. Maddrell), pp. 327–345. Cambridge University Press.

Ellington, C. P. 1980 Vortices and hovering flight. In *Instationäre Effekte an schwingenden Tierflügeln* (ed. W. Nachtigall), pp. 64–101. Wiesbaden: Franz Steiner.

Goldstein, S. 1929 On the vortex theory of screw propellers. *Proc. R. Soc. Lond.* A **123**, 440–465.

Hocking, B. 1953 The intrinsic range and speed of flight of insects. *Trans. R. ent. Soc. Lond.* **104**, 223–345.

Hoff, W. 1919 Der Flug der Insekten und der Vögel. *Naturwissenschaften* **7**, 159–162.

Kármán, T. von & Burgers, J. M. 1935 General aerodynamic theory – perfect fluids. In *Aerodynamic theory* (ed. W. Durand), vol. 2, Div. E. Berlin: Springer.

Kokshaysky, N. V. 1979 Tracing the wake of a flying bird. *Nature, Lond.* **279**, 146–148.

Levy, H. & Forsdyke, A. G. 1927 The stability of an infinite system of circular vortices. *Proc. R. Soc. Lond.* A **114**, 594–604.

Lighthill, M. J. 1973 On the Weis-Fogh mechanism of lift generation. *J. Fluid Mech.* **60**, 1–17.

PHILOSOPHICAL TRANSACTIONS OF THE ROYAL SOCIETY B BIOLOGICAL SCIENCES

PHILOSOPHICAL TRANSACTIONS OF THE ROYAL SOCIETY B BIOLOGICAL SCIENCES

Downloaded from rstb.royalsocietypublishing.org

Magnan, A. 1934 *La locomotion chez les animaux I. Le vol des insectes*. Paris: Hermann et Cie.
Magnan, A., Perrilliat-Botonet, C. & Girard, H. 1938 Essais d'enregistrements cinématographiques simultanées dans trois directions perpendiculaires deux à deux de l'écoulement de l'air autour d'un oiseau en vol. *C.r. hebd. Séanc. Acad. Sci., Paris* **206**, 462–464.
Maxworthy, T. 1979 Experiments on the Weis-Fogh mechanism of lift generation by insects in hovering flight. Part 1. Dynamics of the 'fling'. *J. Fluid Mech.* **93**, 47–63.
Milne-Thomson, L. M. 1973 *Theoretical aerodynamics*. New York: Dover.
Mises, R. von 1959 *Theory of flight*. New York: Dover.
Norberg, R. Å. 1975 Hovering flight of the dragonfly *Aeschna juncea* L., kinematics and aerodynamics. In *Swimming and flying in Nature* (ed. T. Y. Wu, C. J. Brokaw & C. Brennen), vol. 2, pp. 763–781. New York: Plenum Press.
Osborne, M. F. M. 1951 Aerodynamics of flapping flight with application to insects. *J. exp. Biol.* **28**, 221–245.
Pennycuick, C. J. 1968 Power requirements for horizontal flight in the pigeon *Columba livia*. *J. exp. Biol.* **49**, 527–555.
Pennycuick, C. J. 1975 Mechanics of flight. In *Avian biology* (ed. D. S. Farner & J. R. King), vol. 5, pp. 1–75. London: Academic Press.
Phlips, P. J., East, R. A. & Pratt, N. H. 1981 An unsteady lifting line theory of flapping wings with application to the forward flight of birds. *J. Fluid mech.* **112**, 97–125.
Prandtl, L. 1919 Appendix to A. Betz. Schraubenpropellers mit geringstem Energieverlust. *Nachr. Ges. Wiss. Göttingen*, pp. 213–217.
Prandtl, L. & Tietjens, O. G. 1957*a* *Fundamentals of hydro- and aeromechanics*. New York: Dover.
Prandtl, L. & Tietjens, O. G. 1957*b* *Applied hydro- and aeromechanics*. New York: Dover.
Rayner, J. M. V. 1979*a* A vortex theory of animal flight. Part 1. The vortex wake of a hovering animal. *J. Fluid Mech.* **91**, 697–730.
Rayner, J. M. V. 1979*b* A vortex theory of animal flight. Part 2. The forward flight of birds. *J. Fluid Mech.* **91**, 731–763.
Rayner, J. M. V. 1979*c* A new approach to animal flight mechanics. *J. exp. Biol.* **80**, 17–54.
Siekmann, J. 1963 On a pulsating jet from the end of a tube, with application to the propulsion of certain aquatic animals. *J. Fluid Mech.* **15**, 399–418.
Tucker, V. A. 1973 Bird metabolism during flight: evaluation of a theory. *J. exp. Biol.* **58**, 689–709.
Weis-Fogh, T. 1973 Quick estimates of flight fitness in hovering animals, including novel mechanisms for lift production. *J. exp. Biol.* **59**, 169–230.
Wood, J. 1970 A study of the instantaneous air velocities in a plane behind the wings of certain Diptera flying in a wind tunnel. *J. exp. Biol.* **52**, 17–25.
Wood, J. 1972 An experimental determination of the relationship between lift and aerodynamic power in *Calliphora erythrocephala* and *Phormia regina*. *J. exp. Biol.* **56**, 31–36.

PHILOSOPHICAL TRANSACTIONS OF THE ROYAL SOCIETY B BIOLOGICAL SCIENCES
PHILOSOPHICAL TRANSACTIONS OF THE ROYAL SOCIETY B BIOLOGICAL SCIENCES